An Approach to Linear Model-based Testing for Nonlinear Cascaded Mixed-Signal Systems

Reik Müller*, Carsten Wegener†, Hans-Joachim Jentschel*, Sebastian Sattler† and Heinz Mattes†
*Technische Universität Dresden, Germany; {Reik.Mueller, Hans-Joachim.Jentschel}@tu-dresden.de
†Infineon Technologies, Munich, Germany; {Sebastian.Sattler, Heinz.Mattes}@infineon.com

***Abstract*—Linear Model-based Test and Diagnosis (MbT&D) has been successfully applied to single-block modules like Digital-to-Analog Converters (DACs) with a static non-linear transfer characteristic. For Multi-block modules, a diagnosis methodology is needed that can deal with cascades of several linear and non-linear blocks.**

In contrast to non-linear methods, linear MbT&D methods only require matrix operations associated with relatively low computational effort. A modification of the linear MbT&D in combination with Volterra series is presented that can be applied to cascaded non-linear systems, for example, a DAC followed by a low-pass filter. A simultaneous identification of numerous frequency domain Volterra kernels is enabled, and thus, to test the compliance to data sheet specifications.

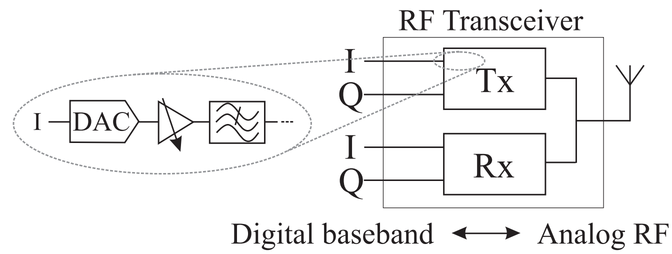

Fig. 1. Typical RF transceiver architecture with transmit (Tx) and receive (Rx) paths. Encircled are the baseband blocks DAC, amplifier, and low-pass filter of the I-channel of the transmit path.

I. Introduction

An RF transceiver, as shown in Fig. 1, is a typical example of a mixed-signal circuit used in wireless communication systems. It consists of a cascade of functional blocks such as amplifiers, mixers and filters. The realization as Systems-on-Chip (SoC) or System-in-Package (SiP) accommodates the drive for increased system integration, while a SiP offers the option of mixing fabrication technologies on a block-by-block basis for optimizing system performance and cost.

Even if efficient test and diagnosis strategies are available for individual standalone blocks, e.g. data converters [1], [2] and linear filters [3], [4], the limited access to internal nodes poses a significant test problem.

One alternative to block-level test is to perform specification oriented system-level tests, which require a full functional test of the system properties – but the increasing number of specification values, summarized in a system specification, and the complexity of their measurement has led to ever-increasing test time and test costs [5].

We aim for a structural test strategy [6], [7] that exploits the knowledge of the system structure. When this structure is represented by a parameterizable model, we call this strategy "Model-based Test" (MbT) [8], [9], [10]. Pass/fail decisions are made by comparing the system performance parameters (like Total Harmonic Distortion, Third-Order Intercept Point, etc.) of the model with the specification. The performance parameters of the the Device Under Test (DUT) are computed from the parameters of the model, identified by key measurements on the DUT. The number of the key measurements is less than the number of measurements, which would be necessary measuring the performance parameters directly on the DUT. Moreover, the model parameters can be used for model-based fault diagnosis [1], [4], [11].

Various MbT methods have been developed by a number of research groups world wide. In [12], an RF subsystem is modeled by applying multivariate adaptive regression splines. Linear MbT was originally proposed in [13] by the National Institute of Standards and Technologies (NIST) and has been introduced in high-volume production [14] in order to reduce the cost of testing an 11-bit video-DAC architecture. In [8] an Artificial Neural Network (ANN) has been applied to model a direct conversion receiver. A comparison of a direct implementation of the NIST approach and a Wavelet based method applied to a single-block programmable gain amplifier is given in [15].

In the present work, linear MbT is made applicable utilizing frequency domain Volterra series [16], which offers the interpretation of model parameters in order to estimate numerous DUT performance parameters at once [17]. As a consequence test time and thus, test costs can be reduced. A simultaneous identification of multiple Volterra kernels is realized by applying only one multi-tone test signal, but differs from other measurement techniques with multi-tone test signal [18], [19].

The paper starts in Sec. II with an explanation of Model based Test and Diagnosis. Afterwards, in Sec. III the DUT is introduced and the identification of the system model parameters as well as the creation of the system model follow in Sec. V and IV, respectively. The verification of the model parameter identification is given in Sec. VI and VII. The calculation of performance parameters of the DUT from identification results is shown in Sec. VIII. Sec. IX concludes the paper.

978-3-9810801-5-5/DATE09 © 2009 EDAA

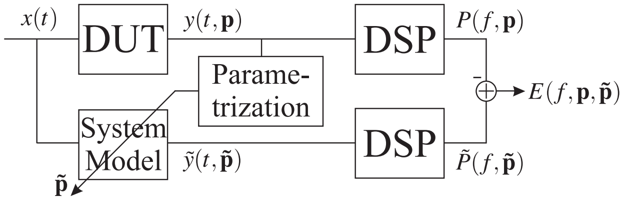

Fig. 2. General block diagram for Model-based Testing; the prediction error signal $E(f,\mathbf{p},\tilde{\mathbf{p}})$ is calculated from the test signal responses $y(t,\mathbf{p})$ and $\tilde{y}(t,\tilde{\mathbf{p}})$.

II. Test and Diagnosis

A. Model-based Test

Assume a physical device has to be tested. Numerous system level tests would have to be performed on a device realized as a SiP with complex system structure. The effort of such a time consuming test can be reduced by applying Model-based Test (MbT). Fig. 2 shows the general structure of MbT.

For MbT, a system model of the DUT is created. The model has a set of ν parameters, denoted by a parameter vector

$$\tilde{\mathbf{p}} = [\tilde{p}_0, \ldots, \tilde{p}_{\nu-1}]^T, \tag{1}$$

while the DUT has a set of μ true parameters, denoted by a parameter vector

$$\mathbf{p} = [p_0, \ldots, p_{\mu-1}]^T. \tag{2}$$

The structure and the number of parameters of the DUT and of the system model do not have to be identical. The model is intended to imitate the Input/Output (I/O) behavior of the DUT. Ideally, the model structure is such, that the I/O behavior of the DUT is matched. The system model parameters have to be determined by applying only a small set of measurements on the DUT using the test signal $x(t)$. The parameter identification is performed by the parametrization block (Fig. 2) based on the response $y(t,\mathbf{p})$ of the DUT.

The output signal $\tilde{y}(t,\tilde{\mathbf{p}})$ of the parameterized system model can be postprocessed in the same way as it is done with the DUT response (DSP blocks). Hence, measurements on the DUT can be replaced by using the system model. In our case the DSP blocks calculate the power spectra $P(f,\mathbf{p})$ and $\tilde{P}(f,\tilde{\mathbf{p}})$ of the DUT and system model responses in order to calculate an error signal $E(f,\mathbf{p},\tilde{\mathbf{p}})$ for rating the parameter identification accuracy.

Having the correct system model parameter set $\tilde{\mathbf{p}}$, DUT-hardware measurements can be replaced by computations utilizing the system model in order to determine the performance parameter values of the DUT. Thus, from the known performance parameter values, a test decision can be obtained in the conventional way. The accuracy of the MbT depends on the capability of the system model to reproduce the I/O behavior of the DUT and on the accuracy of the parameter identification. A more detailed description of MbT is given in [10], [20].

B. Model-based Diagnosis

The system model is derived from the DUT, taking its specific structure into account. Hence, there is a relationship between the system model parameters and the DUT parameters. Thus, the MbT approach offers a capability to identify the root causes of performance degradations.

If the parameter vector $\tilde{\mathbf{p}}$ of the system model is identified by applying MbT to a specific DUT, the parameters $\tilde{p}_i$ and the associated system model blocks, causing the performance degradation, can be localized. There is a relationship between the system model parameter set $\tilde{\mathbf{p}}$ and DUT parameters p_j associated with dedicated DUT blocks. Hence, the system model parameters, that indicate a performance degradation, identify the degraded DUT blocks.

As an example in [21] and [11] descriptions of diagnosing hard faults and parametric deviations for data converters, based on linear MbT, are given.

C. Prediction Error

The MbT approach requires a sufficiently detailed and accurate model. Assuming that we can obtain such a model, the advantage of this approach is that the test and diagnosis tasks are reduced to a model parameter identification problem.

In general, the determined parameters deviate from the ideal parameters, for the system model to imitate the DUT in the best way. Applying identical input signals results in output signals of DUT and system model, which differ from each other. Therefore, a figure of merit is necessary in order to rate the accuracy of the parameter identification.

Fig. 2 shows the block diagram for the evaluation of the response mismatching between a DUT and a system model. A test signal $x(t)$ is applied to the parameterized system model and the DUT and yield in the responses $\tilde{y}(t,\tilde{\mathbf{p}})$ and $y(t,\mathbf{p})$, respectively. The output signals are post processed to the corresponding power spectra $\tilde{P}(f,\tilde{\mathbf{p}})$ and $P(f,\mathbf{p})$ in order to obtain the prediction error signal as defined in [20]:

$$E(f,\mathbf{p},\tilde{\mathbf{p}}) = \tilde{P}(f,\tilde{\mathbf{p}}) - P(f,\mathbf{p}). \tag{3}$$

In our case of prediction error calculation, the DSP blocks in Fig. 2 accomplish a Fast Fourier Transformation (FFT) and convert the amplitude spectrum to a power spectrum.

Several DUTs of the same structure differ in their parameter sets $\mathbf{p}^k$, where k indicates the k-th DUT and thus, the k-th parameter set. Ideally, after tuning the associated parameter set $\tilde{\mathbf{p}}^k$ for a DUT, the prediction error signal $E(f,\mathbf{p}^k,\tilde{\mathbf{p}}^k)$ is zero for every arbitrary input signal $x(t)$.

Because noise is not predictable in power spectrum and we are only interested in significant spectral lines resulting from the deterministic input signal, we define a set F of relevant spectral lines in the output power spectra. Frequency bins, with pure noise and no signal contributions, are excluded from the prediction error calculation. The worst case value of the relevant frequencies in the prediction error signal of a specific DUT defines the prediction error:

$$E_{\max}(\mathbf{p},\tilde{\mathbf{p}}) = \max_{\forall f_i \in F} \|E(f_i,\mathbf{p},\tilde{\mathbf{p}})\|. \tag{4}$$

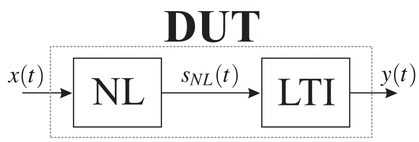

Fig. 3. The Device Under Test as cascade of a nonlinear block followed by an LTI-filter. The internal signal $s_{\mathrm{NL}}(t)$ is not accessible.

TABLE I
NOMINAL DUT PARAMETERS.

Parameter	p_0	p_1	p_2	p_3	p_4
Value	0.50	10.00	0.05	-0.01	$1/(2\pi\cdot 100\,\mathrm{Hz})$

The smaller $E_{\max}(\mathbf{p},\tilde{\mathbf{p}})$ is, the better the system model approximates the DUT with respect to the performance measure that would result from a test signal response from raw DUT measurements.

III. DUT DESCRIPTION

In Fig. 1 the first stages in the Tx path of an RF transceiver are encircled. This subsystem consists of three devices: a DAC, followed by an amplifier and a low pass filter. This cascade converts the digital input signal to the analog domain in preparation for the subsequent up-conversion to the RF domain.

The observation of effects concerning MbT does not necessitate a realistic DUT. That is why our DUT is confined to the baseband function of one Tx path in Fig. 1. In the following, the DUT is reduced to a two block device as depicted in Fig. 3. It consists of a static Non-Linearity (NL) followed by an LTI filter. The nonlinear block is intended to mimic the behavior of both together, the DAC and the amplifier. Gain and nonlinear distortions are set by parameters in the equation for the static nonlinear block:

$$s_{\mathrm{NL}}(t) = p_0 + p_1 x(t) + p_2 x^2(t) + p_3 x^3(t). \tag{5}$$

The functionality of the smoothening filter is represented by a passive LTI filter with the frequency domain characteristic

$$Y(s) = \frac{1}{1+p_4 s} S_{\mathrm{NL}}(s) = G(s) S_{\mathrm{NL}}(s). \tag{6}$$

The signals $S_{\mathrm{NL}}(s)$ and $Y(s)$ denote the Laplace transforms of the input and output signals of the LTI block. According to Eq. (6) the LTI block realizes a first-order low pass filter.

The entire parameter set can be summarized in a parameter vector

$$\mathbf{p} = [p_0,\ p_1,\ \ldots,\ p_4]^T. \tag{7}$$

The DUT has five parameters, with the nominal (design) values listed in Table I. The 3 dB cut-off frequency of the LTI filter is 100 Hz. This set is denoted in the following by the nominal parameter vector $\mathbf{p}^0$.

IV. SYSTEM MODEL

The system model block in Fig. 2 is a model, which is derived from the block structure of the DUT. As in [20] and [22] different system models have been combined with linear MbT, the time domain Volterra model (applied as system model) yields the highest parameter identification accuracy. Hence, the Volterra series approach [16] offers a convenient way to apply linear MbT to our DUT.

The limited interpretability of time domain Volterra kernels motivates a frequency domain Volterra kernel identification. Moreover, the frequency domain is the common data format in RF-measurement pratice and the nonlinearity of the DUT is of limited order, which consequently limits the length of the frequency domain Volterra series. This series is used to represent the system model block (Fig. 2).

The nonlinear block of the DUT is characterized by a Volterra series:

$$\begin{aligned} S_{\mathrm{NL}}(f) = {} & H_{\mathrm{NL},0}(f) + H_{\mathrm{NL},1}(f)X(f) \\ & + \int_{-\infty}^{\infty} H_{\mathrm{NL},2}(f_1, f-f_1) X(f_1) X(f-f_1)\,\mathrm{d}f_1 \\ & + \int_{-\infty}^{\infty}\int_{-\infty}^{\infty} H_{\mathrm{NL},3}(f_1, f_2, f-f_1-f_2) \\ & \quad X(f_1)X(f_2)X(f-f_1-f_2)\,\mathrm{d}f_1\,\mathrm{d}f_2 \end{aligned} \tag{8}$$

with

$$H_{\mathrm{NL},0}(f) = p_0 \delta(f) \tag{9}$$

$$H_{\mathrm{NL},n}(f_1,\ldots,f_n) = p_n \quad \text{for } n = 1,2,3. \tag{10}$$

The frequency domain Volterra kernels of the nonlinear block are denoted by $H_{\mathrm{NL},n}(f_1,\ldots,f_n)$ and the input signal in frequency domain is denoted by $X(f)$. The frequency domain Dirac Delta is denoted by $\delta(f)$ and the transfer function of the LTI-Filter block is denoted by $G(f)$. Hence, the relationship between the LTI-filter input signal and DUT output signal is:

$$Y(f) = H_{\mathrm{LTI},1}(f) S_{\mathrm{NL}}(f) = G(f) S_{\mathrm{NL}}(f). \tag{11}$$

The elimination of S_{NL} yields the resulting Volterra series. Because only harmonic input signals are intended to be used, the frequency domain representation consists of Dirac deltas. Because of the sifting property of the Dirac delta, the integrals in Eq. (8) turn into sums. Then, the resulting Volterra series, which exactly imitates the I/O characteristic of the DUT is

$$\begin{aligned} Y(f) = {} & H_0(f) + H_1(f)X(f) + \\ & \sum_{f_1=-\infty}^{\infty} H_2(f_1, f-f_1) X(f_1) X(f-f_1) + \\ & \sum_{f_1=-\infty}^{\infty}\sum_{f_2=-\infty}^{\infty} H_3(f_1, f_2, f-f_1-f_2) X(f_1) \\ & \cdot X(f_2) X(f-f_1-f_2) \end{aligned} \tag{12}$$

where

$$H_0(f) = G(f)p_0\delta(f) \quad (13)$$
$$H_1(f) = G(f)p_1 \quad (14)$$
$$H_n(f_1,\ldots,f_n) = G(f_1+\cdots+f_n)p_n\,; \quad n=2,3 \quad (15)$$

and

$$f = f_1+\cdots+f_n \quad (16)$$
$$G(f) = G(f_1+\cdots+f_n). \quad (17)$$

Eqs. (13)–(15) describe the relationship between the DUT parameter set $\mathbf{p}$ and the system model parameter set $\tilde{\mathbf{p}} = [H_0 \ldots H_{\nu-1}]^T$:

$$\tilde{\mathbf{p}} = f(\mathbf{p}). \quad (18)$$

V. System Model Parameter Identification

The system model parameter identification is realized by the parameterizing-block depicted in Fig. 2. The parametrization is intended to be realized using a linear model [13], [21], because it promises an accurate and fast parameter identification.

The linear model is realized and used as follows. For $f_i \in F$, the DUT's output spectrum $Y(f_i,\mathbf{p})$ is written as a vector $\mathbf{b}$. A linear system of equations is created modeling the relationship between the vector $\mathbf{b}$ and the nominal DUT output amplitudes $Y(f_i,\mathbf{p}^0)$ in a vector $\mathbf{b}^0$:

$$\mathbf{b} = \mathbf{A}_{\text{est}}\tilde{\mathbf{x}} + \mathbf{b}^0. \quad (19)$$

The vector $\tilde{\mathbf{x}} \in \mathbb{C}^l$ represents the parameters of the linear model. The matrix $\mathbf{A}_{\text{est}}$ is a model matrix which provides the relationship between the model vector $\tilde{\mathbf{x}}$ and the complex DUT output signal amplitudes $Y(f_i,\mathbf{p})$.

A second model matrix $\mathbf{A}_{\text{pred}}$ is used to predict the system model parameter set $\tilde{\mathbf{p}}$ which depends on the model parameter set $\tilde{\mathbf{x}} \in \mathbb{C}^l$ as follows:

$$\tilde{\mathbf{p}} = \mathbf{A}_{\text{pred}}\tilde{\mathbf{x}} + \tilde{\mathbf{p}}^0. \quad (20)$$

Because the vector $\mathbf{b}$ represents measurement values, the parameter set $\tilde{\mathbf{p}}$ is predicted as an approximation of the DUT parameter set $\mathbf{p}$ utilizing both matrices $\mathbf{A}_{\text{est}}$ and $\mathbf{A}_{\text{pred}}$. The matrix $\mathbf{A}_{\text{pred}}$ provides the relationship between the model vector $\tilde{\mathbf{x}}$ and the system model parameter set $\tilde{\mathbf{p}}$.

The matrices $\mathbf{A}_{\text{est}}$ and $\mathbf{A}_{\text{pred}}$ are created from "noise-free" measurements of the system model parameters (Volterra kernels [18], [19]) and from the test signal responses for a subset of the DUTs in run up of the production test. The generation of the linear model matrices is explained in detail in [10].

VI. Simulation Setup

A. DUT and System Model Setup

As done in [20] and [22], two sets of DUTs are created. Each DUT k has its individual parameter set $\mathbf{p}^k$. The parameters p_i^k are Gaussian distributed around the nominal parameter values p_i^0 with a standard deviation of 1% in the first set and 10% in the second set.

There are some changes in the general MbT-setup shown in Fig. 2: The system model block is replaced by the frequency domain Volterra model (Sec. IV), which requires a frequency domain input signal $X(f)$, while the DUT input signal $x(t)$ is in time domain. The parametrization block applies the linear model from Sec. V and uses the frequency domain output signal from the DUT in order to estimate the Volterra kernels of the system model.

The outputs of DUT and system model are post-processed in order to obtain the output spectra and the prediction error $E_{\max}(\mathbf{p},\tilde{\mathbf{p}})$ for rating the model accuracy.

TABLE II
Multi-tone test signal definition.

$f/_{\text{Hz}}$	70	80	91	103	116	149	200
$\phi/_{\text{rad}}$	2.21	0.70	0.75	4.49	4.73	0.69	5.99

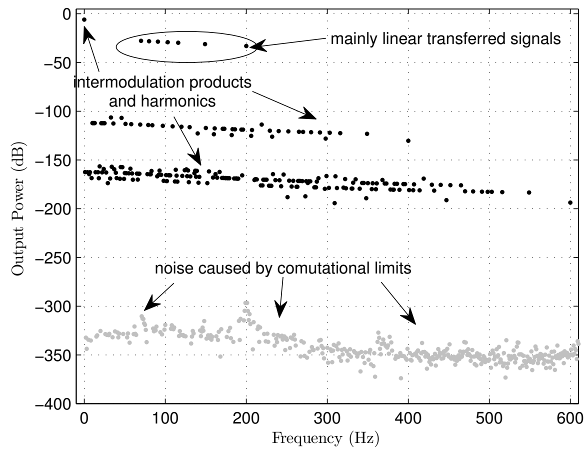

Fig. 4. Power spectrum $P(f,\mathbf{p}^0)$ of the response $y(t,\mathbf{p}^0)$ of the DUT with nominal parameters.

B. Test Signal

A general frequency dependency inhere in the Volterra kernels: $H_n(f_1,\ldots,f_n)$. Assume, there is a test signal with a finite number of harmonics. The variation of the harmonic's frequencies determines such Volterra kernels, which contributes to the test signal response. Hence, only those Volterra kernels can be identified, which are addressed by the test signal harmonics. The parameter identification using the linear modeling allows the simultaneous identification of all addressed Volterra kernels. Thus, a multi-tone test signal can be used

$$x(t) = \sum_{l=1}^{7} A_l \cos\left(2\pi f_l t + \phi_l\right). \quad (21)$$

In our case, it consists of seven frequency components as detailed in Table II. The amplitudes of the sine waves comprising this test signal are all equal, thus $A_l = 10$ mV.

The simulation of the DUT results in a steady-state response, which is sampled at a rate of $f_s = 16.384$ kHz for the duration of one second. After applying an FFT to the output signal a power spectrum is obtained as shown in Fig. 4. The frequency resolution is $f_0 = 1$ Hz and the spectral lines are located at $f = m \cdot f_0$, with integer numbers m.

VII. Identification Results

A. Previous Work

In [20], two identification methods have been applied to the DUT in Fig. 3 with the system model and the DUT structure being identical. A very time consuming nonlinear optimization yield the system model parameter set $\tilde{\mathbf{p}}$ associated with a small prediction error of 10^{-7} dB, limited only by computation inaccuracies. In contrast, the fast parameter identification using the linear modeling (Sec. V) yield large prediction errors of approximately 10^{-5} dB and 10^{-3} dB for a 1% and a 10% DUT parameter standard deviation, respectively.

In [22], a time domain Volterra model as system model successfully enabled the application of linear modeling to a time domain version of the DUT. The prediction error was smaller than 10^{-8} dB.

B. Simulation Results

According to Sec. VI two sets of DUTs have been created with a 1% and 10% standard variation from the nominal DUT parameters. With the setup shown in Fig. 2 the linear parameter identification procedure from Sec. V was used to estimate the frequency domain Volterra kernels of each DUT in both sets.

The prediction error $E_{\max}(\mathbf{p}^k, \tilde{\mathbf{p}}^k)$ has been calculated from the output signal of each DUT k and of the output signal corresponding system model – parametrized by the identified Volterra kernels. The mean prediction error over all DUTs in each set is depicted in Fig. 5 and is marked with dots and circles for a standard variation of 1% and 10%, respectively. It settles at about 10^{-6} dB for both sets.

The model order l defines the length of the linear model vector $\tilde{\mathbf{x}}$ in Eq. (19) and, thus, indicates the computational effort to calculate the system model parameters from the DUT response. In case of 1% standard variation, there is only a model order of $l = 13$ necessary. In case of 10% standard variation a model order of $l = 22$ is needed to reach the minimum prediction error. Increasing the model order does not result in lower prediction errors.

For comparison, the best prediction error reached in [22] for a time domain Volterra kernel identification is $2.1 \cdot 10^{-9}$ dB and is marked by a dash-dotted line in Fig. 5.

The frequency domain Volterra kernel estimation is degraded in accuracy in comparison to the time domain Volterra kernel identification. Within the noiseless consideration of the signals, the accuracy of the parameter identification is only influenced by the computational accuracy. One drawback calculating the output signal from frequency domain Volterra kernels is, that numerous Volterra kernels and powers of input signal amplitudes have to be multiplied and accumulated. Because both can differ by orders of magnitude, the computational accuracy can be deficient and large prediction errors may result.

VIII. DUT Performance

The multi-tone test signal response provides information about the DUT performance parameters which traditionally would be sequentially measured with numerous single- and two-tone measurements. Such measures would be e.g. Total Harmonic Distortion (THD), Spurious-Free Dynamic Range, Third-order Intercept Point (IP3), etc.

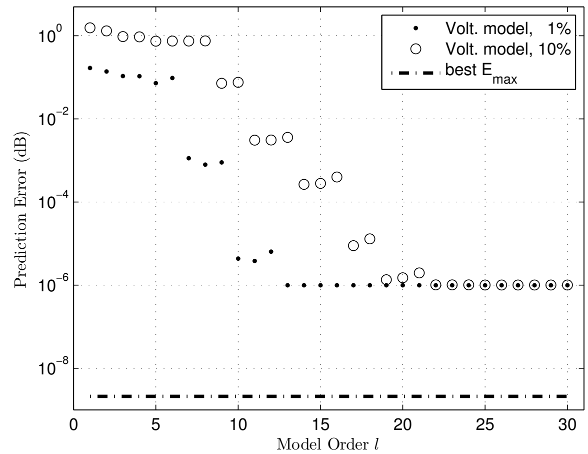

Fig. 5. Mean prediction error of a set of 100 DUTs with a standard deviation from nominal parameter values of 1% and 10%, respectively. The resimulation was realized using the frequency domain Volterra model. The dashed line marks the minimum prediction error reached in [22].

A concrete example of THD calculation was shown in [20], where a seven-tone test signal, designed for multi-tone THD estimation, had been applied. There, the THD for a specific excitation frequency is defined as

$$THD(f,\mathbf{p}) = 10\log_{10}\frac{|Y(f,\mathbf{p})|^2}{\sum\limits_{i=2}^{3}|Y(i\cdot f,\mathbf{p})|^2}\ \text{dB} \tag{22}$$

and evaluates in 95.0227 dB for our DUT at a frequency of 70 Hz for the nominal parameter set $\mathbf{p}^0$ and the multi-tone test signal as specified in Sec. VI-B. An equivalent single-tone measurement yields a THD of 95.0223 dB.

Instead of applying measurements to the DUT or making simulations with the system model, performance parameters like THD and IP3 can be directly calculated from Volterra kernels [23], [17]. Then, the THD as defined in [20] is calculated:

$$THD(f,\mathbf{p}) \approx 10\log_{10}\frac{|H_1(f,\mathbf{p})X(f)|^2}{\sum\limits_{i=2}^{3}|H_i(\underbrace{f,\ldots,f}_{i\text{-times}},\mathbf{p})X^i(f)|^2}. \tag{23}$$

Where $X(f)$ is the complex amplitude of the virtual single-tone test signal at the specific test frequency f and $|X(f)| = A_0/2$. With the Volterra kernels of the nominal DUT follows a THD of 95.0223 dB. Inherently, there is a small systematic error in Eq. (23), because the third order contributions to the amplitude at the frequency f are neglected.

For each DUT of the sets from Sec. VI-A the THD has been calculated using the predicted Volterra kernels ($\rightarrow THD_V$) from multi-tone measurement and applying single-tone measurements ($\rightarrow THD_M$). In both cases the test frequency was 70 Hz. Fig. 6 shows the mean difference $\Delta THD = |THD_V - THD_M|$ vs. the model order over

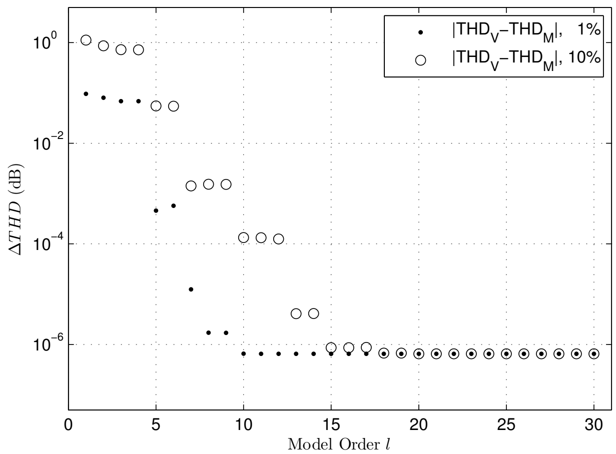

Fig. 6. Mean difference $|THD_V - THD_M|$ versus model order l for a set of 100 DUTs with a standard deviation for the nominal parameter values of 1% and 10%, respectively.

100 DUTs. With increasing model order the value of ΔTHD decreases. This behavior corresponds with the prediction error shown in Fig. 5. For both sets of DUTs ΔTHD settles at 10^{-6} dB.

In contrast to the single-tone THD measurement, the multi-tone based estimation of the Volterra kernels also provides information about the intermodulation properties (e.g. IP3), which can be calculated from the simultaneous estimated additional Volterra kernels [23].

IX. Conclusion

For evaluating the accuracy of Model-based Test and Diagnosis methodologies the prediction error as a figure of merit has been introduced. Exemplary for a cascaded DUT topology of a DAC followed by a filter a linear MbT method has been presented, which allows to estimate simultaneously numerous frequency domain Volterra kernels with low prediction error – using only one multi-tone test signal. The kernel identification is reduced to one measurement associated with solving a linear system of equations of 13 to 22 unknown complex variables, with dependency from the DUT parameter standard variation.

Identifying frequency domain Volterra kernels can be used for Model-based Test of the DUT's compliance to data sheet specifications. In addition, the Volterra modeling approach allows us to achieve the same quality of the test and diagnosis as obtained for nonlinear identification methods, but at a fraction of the computational cost.

Acknowledgment

This work has been supported by the German government (BMBF) in project Dionysys within the research promotion program IKT 2020 under grant No. 01 M 3084.

References

[1] E. Liu, W. Kao, E. Felt, and A. Sangiovanni-Vincentelli, "Analog testability analysis and fault diagnosis using behavioral modeling," in *Proc. CICC*, ser. Custom Integrated Circuits Conference, May 1994, pp. 413 – 416.

[2] M. Wagdy, "Diagnosing ADC nonlinearity at the bit level," *Trans. on Instr. amd Meas.*, vol. 38, no. 6, pp. 1139–1141, Dec. 1989.

[3] J. Bandler and A. Salama, "Fault diagnosis of analog circuits," *Proc. IEEE*, vol. 73, no. 8, pp. 1279–1325, Aug. 1985.

[4] A. Biasizzo and F. Novak, "A methodology for model-based diagnosis of analog circuits," *Applied Artificial Intelligence*, vol. 14, pp. 253–269, 2000.

[5] ITRS, "International technology roadmap for semiconductors," Sematech, Tech. Rep., 2007.

[6] G. Devarayanadurg, M. Soma, P. Goteti, and S. Huynh, "Test set selection for structural faults in analog IC's," *Trans. CAD of ICs and Systems*, vol. 18, no. 7, pp. 1026–1039, July 1999.

[7] A. Majhi, K. Agrawal, and D. Vishwani, "Mixed-signal test," in *Proc. VLSI Design*, ser. Int. Conf. on VLSI Design, Jan. 1998, pp. 285–288.

[8] L. Barford, N. Tufillaro, S. Jefferson, and A. Khoche, "Model-based test for analog integrated circuits," in *Proc. IMTC*, ser. IEEE Instr. and Meas. Tech. Conf., Warsaw, Poland, May 2007, pp. 1–6.

[9] E. Felt and A. Sangiovanni-Vincentelli, "Testing of analog systems using behavioral models and optimal experimental design techniques," in *Proc. ICCAD*, ser. Int. Conf. on Computer-Aided Design, Nov. 1994, pp. 672 – 678.

[10] C. Wegener and M. Kennedy, "Linear model-based testing of ADC nonlinearities," *Trans. on Circuits and Systems I*, vol. 51, no. 1, pp. 213–217, Jan. 2004.

[11] ——, "Hard-fault detection and diagnosis during the application of model-based data converter testing," *Journal of Electronic Testing: Theory and Applications*, vol. 23, no. 6, pp. 513–525, December 2007.

[12] A. Halder, S. Bhattachary, and A. Chatterjee, "Automatic multitone alternate test generation for RF circuits using behavioral models," in *Proc. ITC*, ser. Int. Test Conference, 2003, pp. 665–673.

[13] G. Stenbakken and T. Souders, "Modeling and test point selection for data converter testing," in *ITC*, ser. Int. Test Conf., 1985, pp. 813–817.

[14] D. McSweeney, J. McGovern, C. Wegener, M. Kennedy, L. O'Connel, and J. O'Riordan, "Model-based reduction of DAC test-time," in *Proc. ICTW*, ser. IEEE IC Test Workshop, Limerick, Ireland, September 2004, pp. 75–80.

[15] X. Zhang, S. Ang, and C. Carter, "Test point selections for a programmable gain amplifier using NIST and wavelet transform methods," in *Proc. ATS*, ser. Asian Test Symposium, Bejing, China, October 2007, pp. 230–238.

[16] S. Boyd, L. Chua, and C. Desoer, "Analytical foundations of volterra series," *IMA Journal of Mathematical Control & Information*, pp. 243–282, 1984.

[17] A. Bauer and W. Schwarz, "Circuit analysis and optimization with automatically derived volterra kernels," in *ISCAS*, ser. IEEE International Symposium on Circuits and Systems, May 2000, pp. 491–494.

[18] S. Boyd, Y. Tang, and L. Chua, "Measuring volterra kernels," *IEEE Trans. on Circuits and Systems*, vol. 30, no. 8, pp. 571–577, Aug. 1983.

[19] C. Evans, D. Rees, L. Jones, and M. Weiss, "Periodic signals for measuring nonlinear volterra kernels," *IEEE Trans. on Instrumentation and Measurement*, vol. 45, no. 2, pp. 362–371, April 1996.

[20] R. Müller, C. Wegener, and H.-J. Jentschel, "An approach to model-based testing of mixed-signal sips," in *Proc. 14th IEEE IMS3TW*, ser. IEEE International Mixed-Signals, Sensors and Systems Test Workshop, Vancouver, Canada, June 2008.

[21] C. Wegener and M. Kennedy, "Linear model-based error identification and calibration for data converters," in *Proc. DATE*, ser. Design, Automation and Test in Europe Conf., Munich, Germany, March 2003, pp. 630–635.

[22] R. Müller, C. Wegener, H.-J. Jentschel, and S. Sattler, "Model-based testing and diagnosis for mixed-signal systems-in-package," in *Zuverlässigkeit und Entwurf 2008, GMM Fachbericht 57*, Ingolstadt, Germany, September 2008, pp. 17–24.

[23] A. Bauer, "Analysis methods for nonlinear electronic circuits and systems based on volterra series," Ph.D. dissertation, Technische Universität Dresden, 2004.